Micro Nano Bio Aspects

https://www.mnba-journal.com

Online ISSN: 2980-8081

Docking of helicase, main protease, papain-like protease, and RNA-dependent RNA polymerase of SARS-CoV-2 by theaflavin-3-gallate

Qassim Hassan Aubais Aljelehawy

Department of Chemistry, College of Education, University of Al-Qadisiyah, Iraq

ARTICLE INFO

Original paper

Article history:
Received: 07 Aug 2023
Revised: 23 Aug 2023
Accepted: 23 Aug 2023
ePublished: 10 Sept 2023

Keywords:
Theaflavins, Polyphenols, Theaflavin-3-gallate, Oolong tea, Black tea, Helicase NSP13

ABSTRACT

Polyphenol phytochemicals have obtained huge attention owing to their numerous therapeutic applications. Green, oolong, and black teas are the main sources of abundant polyphenols. Theaflavins are a large group of polyphenols isolated from oolong and black tea. Theaflavins have shown various therapeutic advantages, specifically antimicrobial activity. Hear, the antiviral effect of theaflavin-3-gallate as one the main theaflavins against severe acute respiratory syndrome coronavirus 2 (SARS‑CoV‑2) has been investigated by molecular docking study. This study exhibited the best binding affinity for the interaction of the theaflavin-3-gallate ligand with SARS-CoV-2 helicase NSP13 with a Vina score of -10.3 kcal/mol compared with theaflavin-3-gallate and spike protein S1 complex with a lowest binding affinity of -8.2 kcal/mol. For a better understanding of the antiviral activity of theaflavin-3-gallate compound, experimental *in vitro* and *in vivo* studies about other bioactive compounds and drugs are needed.

DOI: https://doi.org/10.22034/mnba.2023.410567.1042

Introduction

For the improvement of conventional antiviral drugs having side effects, finding novel biocompatible, bioavailable, and biodegradable antiviral agents is necessary [1, 2]. Theaflavins with the chemical formula of $C_{29}H_{24}O_{12}$ are a large group of polyphenols frequently available in oolong and black teas [3]. Theaflavin-3-3'-digallate, theaflavin-3'-gallate, and theaflavin-3-gallate are the main theaflavins, which can be synthesized from the flavan-3-ols in tea leaves by the enzymatic oxidation [4]. Catechins and theaflavins as the major phenolic group have various health advantages including hepatoprotective, neuroprotective, anti-inflammatory, skin protective, anticancer, antioxidant, cardioprotective, anticancer, and antimicrobial effects [5]. In addition, theaflavin-3,3′-digallate remarkably decreased the upregulation of kidney injury molecule-1 and ameliorated renal ischemia/reperfusion injury in the kidney tissues [6]. Investigations into viral infections, specifically coronavirus disease 2019 (COVID-19) have obtained more attention because of it's contagious nature [7]. Many studies have been carried out to develop novel antiviral compounds targeting key protein targets of severe acute respiratory syndrome coronavirus 2 (SARS‑CoV‑2) [8, 9]. In the present study, the antiviral effect of theaflavin-3-gallate as one the main theaflavins against SARS‑CoV‑2) has been investigated by molecular docking study. For this study, viral receptors were the main proteases (M^{pro}; a class of highly conserved cysteine hydrolases in β-coronaviruses), spike protein S1, RNA-dependent RNA polymerase or RNA replicase (RdRp), helicase, and papain-like protease (PL^{pro}) [10-13].

Materials and methods

Theaflavin-3-gallate as a ligand was obtained from the PubChem database (Figure 1a). SARS-CoV-2 helicase NSP13 (PDB code: 6ZSL), spike protein S1 (PDB code: 6M0J, resolution: 2.45 Å), RdRp (PDB code: 6M71), PL^{pro} (PDB code: 3E9S), and M^{pro} (PDB code: 6LU7) were receptors extracted from protein data bank (PDB) (Figures 1b-f). The UCSF Chimera1.12

*Corresponding author. E-mail: qassim.hassan@qu.edu.iq

program was employed to optimize the compounds. The molecular docking study was performed by the CB-Dock server (http://clab.labshare.cn/cb-dock/php/index.php) [14, 15].

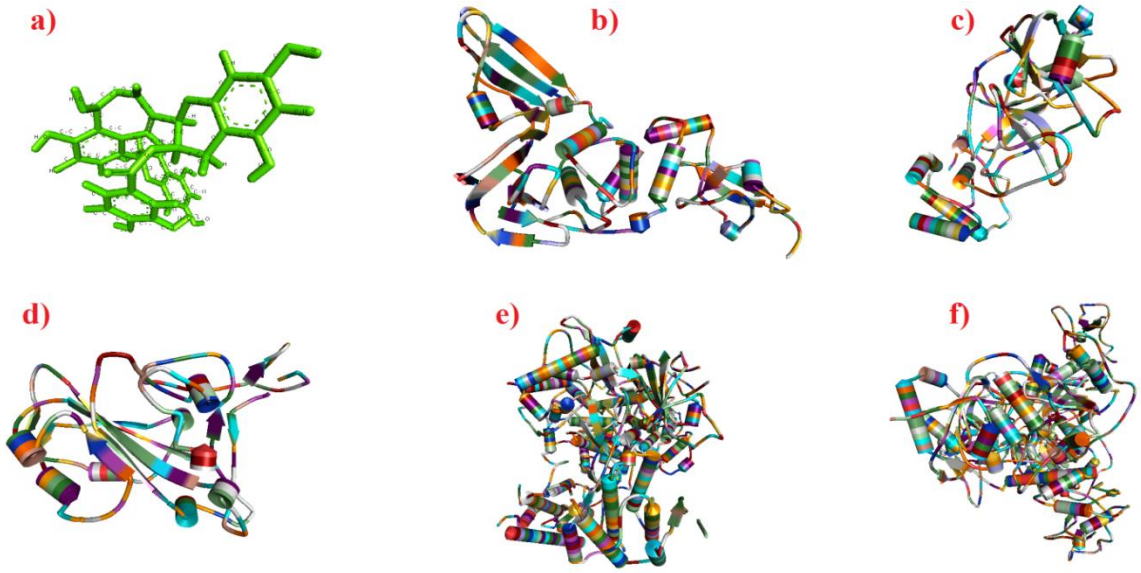

Fig. 1. Chemical and schematic structures of theaflavin-3-gallate (a), 3E9S (b), 6LU7 (c), 6M0J (d), 6M71 (e), and 6ZSL (f).

Results and discussion

CB-Dock showed the highest binding affinity for the interaction of theaflavin-3-gallate ligand and 6ZSL receptor with a Vina score of −10.3 kcal/mol compared to theaflavin-3-gallate and 6M0J receptor with a lowest binding affinity of -8.2 kcal/mol (Tables 1-4). H-bonds were indicated for GLU197, GLN194, and GLN194 in the distances of 1.930, 2.243, and 2.484 Å, respectively (Figure 2).

The molecular docking study showed remarkable interaction between theaflavin 3-gallate and the active site residues of M^{pro} compared to a standard molecule GC373 and theaflavin. M^{pro} protein of SARS-CoV-2 was inhibited by theaflavin 3-gallate in an IC_{50} amount of 18.48 μM [16]. In another study, theaflavin digallate displayed a better docking score of −10.57 compared with adefovirdipivoxil (−8.25), famciclovir (−7.54), tecovirimat (−7.54), darunavir (−7.5), and zidovudine (−7.39) [17]. In a similar study, 14 terpenoids were evaluated for their docking interaction with M^{pro} and SARS-CoV-2 spike targets. In contrast to targeting Spike protein, deacetylnomilin (−8.35), ichangin (−8.40), nomilin (−8.51), and β-amyrin (−8.79) presented suitable energies of interaction with M^{pro} [18].

Table 1. CB-dock results for interaction of theaflavin-3-gallate ligand and 6M0J receptor.

CurPocket ID	Vina score	Cavity volume (Å^3)	Center (x, y, z)	Docking size (x, y, z)	Contact residues
C2	-8.2	112	-26, 31, 32	24, 24, 24	**Chain E**: ARG355 TYR396 PRO426 ASP428 PHE429 THR430 GLY431 LYS462 PRO463 PHE464 SER514 PHE515 GLU516 LEU517 LEU518
C4	-7.3	104	-32, 12, 27	24, 24, 24	**Chain E:** PHE338 GLY339 PHE342 ASN343 ALA344 THR345 ARG346 VAL367 LEU368 SER371 SER373 PHE374 TRP436 LEU441 ARG509
C3	-7.0	106	-37, 43, 13	24, 24, 24	**Chain E:** ARG454 ARG457 LYS458 SER459 ASN460 LEU461 LYS462 GLU465 ARG466 ASP467 ILE468 SER469 GLU471 ILE472 TYR473 PRO491
C5	-6.7	94	-20, 27, 35	24, 24, 24	**Chain E:** GLY381 VAL382 LEU390 PHE392 TYR396 PRO426 ASP428 PHE429 THR430 GLY431 PHE464

CurPocket ID	Vina score	Cavity volume (Å^3)	Center (x, y, z)	Docking size (x, y, z)	Contact residues
					LEU513 SER514 PHE515 GLU516 LEU517 LEU518
C1	-6.5	197	-32, 25, 7	24, 24, 24	**Chain E**: ARG403 GLU406 LYS417 TYR453 LEU455 SER494 TYR495 GLY496 PHE497 GLN498 THR500 ASN501 GLY502 TYR505

Table 1 (continued).

Table 2. CB-dock results for interaction of theaflavin-3-gallate ligand and 3E9S receptor.

CurPocket ID	Vina score	Cavity volume (Å^3)	Center (x, y, z)	Docking size (x, y, z)	Contact residues
C5	-8.8	203	-40, 11, 10	24, 24, 24	**Chain A**: VAL99 GLY100 GLY101 LEU102 GLN122 GLN123 LEU124 GLU125 SER241 PHE242 GLY257 THR258 PHE259 LEU260 THR278 ALA279 LYS280 TYR306 LYS307 GLU308
C3	-8.4	243	-5, 26, 15	24, 24, 24	**Chain A**: PRO60 SER61 ASP63 THR64 ARG66 SER67 GLU68 ALA69 PHE70 GLU71 TYR73 THR75 LEU76 ASP77 GLU78 SER79 PHE80 LEU81
C2	-7.7	647	-28, 21, 28	24, 24, 24	**Chain A**: ASN110 LYS158 GLY161 GLU162 LEU163 GLY164 ASP165 ARG167 GLU168 TYR265 ASN268 TYR269 GLN270 CYS271 TYR274
C4	-7.2	212	-28, 8, 27	24, 24, 24	**Chain A**: TRP107 ASN110 LEU163 GLU264 THR266 GLY267 CYS271 GLY272 HIS273 THR275 ARG285 ASP287 GLY288 ALA289 HIS290
C1	-6.4	712	-8, 12, 9	24, 24, 24	**Chain A**: ASN14 ASP38 GLY39 THR55 PHE57 TYR72 MET85 LEU88 THR91 LYS92 TRP94 PHE96 GLU135 ARG139 ASP144 ALA146 ASN147

Table 3. CB-dock results for interaction of theaflavin-3-gallate ligand and 6LU7 receptor.

CurPocket ID	Vina score	Cavity volume (Å^3)	Center (x, y, z)	Docking size (x, y, z)	Contact residues
C3	-9.1	258	-14, 11, 72	24, 24, 24	**Chain A**: HIS41 THR45 SER46 MET49 TYR54 PHE140 LEU141 ASN142 SER144 CYS145 HIS163 HIS164 MET165 GLU166 LEU167 HIS172 VAL186 ASP187 ARG188 GLN189 THR190 ALA191 GLN192
C1	-7.6	688	-24, 1, 56	24, 24, 24	**Chain A**: ARG131 ASP197 THR198 THR199 TYR237 ASN238 TYR239 LEU271 LEU272 GLN273 GLY275 MET276 ALA285 LEU286 LEU287 GLU288 ASP289 GLU290
C2	-7.4	548	-14, 34, 56	24, 24, 24	**Chain A**: GLU14 GLY15 CYS16 MET17 VAL18 GLN19 TRP31 GLN69 ALA70 GLY71 ASN95 PRO96 LYS97 ASN119 GLY120 SER121 PRO122
C5	-7.2	212	-34, 16, 54	24, 24, 24	**Chain A**: PHE8 LYS102 VAL104 ILE106 GLN107 GLN110 THR111 ASN151 ILE152 ASP153 SER158 CYS160 ILE249 THR292 PRO293 PHE294 ASP295
C4	-7.1	239	-37, 5, 58	24, 24, 24	**Chain A**: VAL104 ARG105 ILE106 GLN107 PRO108 GLY109 GLN110 THR111 PRO132 ASN151 ILE200 VAL202 ASN203 GLU240 THR243 ASP245 HIS246 ILE249 THR292 PRO293

Table 4. CB-dock results for interaction of theaflavin-3-gallate ligand and 6M71 receptor.

CurPocket ID	Vina score	Cavity volume (Å^3)	Center (x, y, z)	Docking size (x, y, z)	Contact residues
C2	-9.3	775	127, 135, 127	24, 24, 24	**Chain A**: ARG249 LEU251 THR252 SER255 ASN314 VAL315 LEU316 SER318 THR319 PRO323 ARG349 GLU350 THR394 CYS395 PHE396 TYR456 ARG457 TYR458 ASN459 LEU460 PRO461 THR462 ASN628 PRO677
C3	-8.6	724	120, 120, 136	24, 24, 24	**Chain A**: ASP452 TYR455 MET542 LYS545 ARG553 ALA554 ARG555 THR556 VAL557 LYS621 CYS622 ASP623 ARG624 THR680 SER682 THR687 ALA688 ASN691 LEU758 SER759 ASP760 ASP761
C4	-6.8	574	146, 132, 82	24, 24, 24	**Chain A**: ARG33 PHE35 LYS50 VAL71 LYS73 ARG74 THR76 ASN79 GLU83 HIS99 ILE114 ARG116 THR206 ASP208 ASN209 TYR217 ASP218 PHE219 GLY220 ASP221
C1	-6.7	1089	122, 139, 100	24, 24, 24	**Chain A**: ASP291 GLN292 THR293 LEU302 ASP303 ARG305 CYS306 HIS309 ARG467 LEU470 ARG735 ASP736 VAL737
C5	-6.1	549	121, 96, 146	24, 24, 24	**Chain A**: PHE429 LYS430 GLU431 GLY432 SER433 GLU436 LEU437 LYS438 PHE440 **Chain C**: LYS2 MET3 SER4 LYS7 LYS43 ASP44 THR45

Table 5. CB-dock results for interaction of theaflavin-3-gallate ligand and 6ZSL receptor.

CurPocket ID	Vina score	Cavity volume (Å^3)	Center (x, y, z)	Docking size (x, y, z)	Contact residues
C1	-10.3	4329	-32, 20, -49	24, 24, 30	**Chain B**: VAL193 GLN194 ILE195 GLY196 GLU197 THR214 THR215 TYR217 THR228 HIS230 PRO335 ALA336 VAL340 GLU341 **Chain A**: PHE182 THR183 TYR185 GLN194 ILE195 GLY196 GLU197 THR214 THR215 THR228 ALA336 ARG337 ALA338 ARG339
C5	-10.1	2002	-32, 29, -75	30, 24, 24	**Chain A**: TYR149 PRO175 ASN177 ASN179 TYR180 PRO408 ARG409 THR410 LEU411 LEU412 THR413 LYS414 GLY415 ASP483 VAL484 SER485 SER486 PRO514 TYR515 ASN516 THR532 ASP534 THR552 ALA553 HIS554 ARG560
C4	-9.7	2136	-16, 35, -64	24, 24, 24	**Chain A**: LYS139 THR141 GLU142 GLU143 PHE145 LYS146 ASN179 TYR180 VAL181 PHE182 THR183 GLU197 LEU227 THR228 SER229 HIS230 CYS309 ARG339 ASN361 THR380 TYR382 ASP383 PRO408 THR410 LEU411
C2	-8.9	3723	-11, 20, -69	24, 32, 35	**Chain A**: LEU138 LYS139 GLU142 GLU143 LYS146 ASN179 TYR180 VAL181 THR228 HIS230 CYS309 SER310 ASN361 GLU375 MET378 THR380 TYR382 ASP383 ALA407 PRO408 ARG409 THR410 ASP534 SER535
C3	-8.8	2984	-23, 20, -21	35, 24, 30	**Chain B**: LYS139 GLU142 GLU143 LYS146 ASN179 TYR180 VAL181 THR228 CYS309 SER310 VAL360 ASN361 MET378 THR380 ASP383 ALA407 PRO408 ARG409 THR410 LEU411 ASP534

There were free binding energy (ΔG) values of −6.7, −6.4, −6.4, −6.3, −7.2, and −6.6 kcal/mol for ligands of eriodictyol, pemirolast, mycophenolic acid, ribavirin, remdesivir, and ritonavir toward M^{pro}, respectively.

Moreover, for angiotensin-converting enzyme 2 (ACE2) receptor, binding energy amounts were −8.2, −8.6, −8.2, −7.3, and −7.5 kcal/mol for ritonavir, lopinavir, remdesivir, pemirolast, and eriodictyol drugs, respectively [19]. Probabilities of binding to active site-pocket were 80% and 70% for mycophenolic acid acyl glucuronide and remdesivir higher than antiviral drugs of avigan (30%), tamiflu (60%), and GRL-0667 (40%) [20]. Carbohydrate-binding agents can target the homotrimeric transmembrane spike glycoprotein of coronaviruses, effectively. In this way, plant lectins and lectin-like mimic pradimicin-A exhibited desirable docking properties against N-linked glycans of SARS-CoV-2 spike glycoprotein. Narcissus pseudonarcissus agglutinin, griffithsin, cyanovirin-N, and banana lectins had docking energies of –269.3, –252.3, –230.9, –219.8 (wild-type) kcal/mol, respectively toward N-linked glycans of SARS-CoV-2 spike glycoprotein [21]. Herbal metabolite can hinder SARS-CoV-2 in safe therapy. For example, Withanoside V related to *Withania somnifera* had the best binding energy (− 83.45 kJ/mol) with M^{pro} compared to withanoside-VI (− 61.97 kJ/mol), racemoside-A (− 56.35 kJ/mol), racemoside-B (− 52.44 kJ/mol), and shatavarin-IX (− 53.99 kJ/mol) [22].

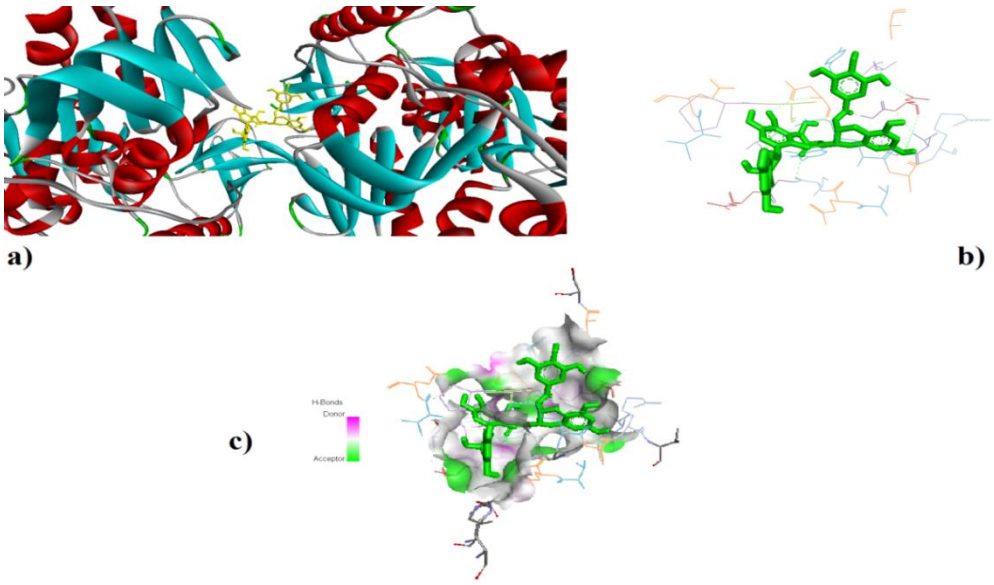

Fig. 2. Docking active site for model 1 obtained by CB-Dock (a), the interaction of amino acids of the SARS-CoV-2 NSP13 helicase with the aflavin-3-gallate compound (b), and the surface around ligand of theaflavin-3-gallate (c).

Conclusions

Many research programs have been carried out to develop novel drugs targeting key protein targets of SARS-CoV-2. Finding and designing safe and effective antiviral agents is time consuming and expensive process. Molecular docking studies and the repurposing of approved compounds can cost-effectively accelerate this process. The highest binding affinity was found for the interaction of theaflavin-3-gallate ligand towards helicase receptor than to theaflavin-3-gallate and spike protein S1 receptor with the lowest binding affinity. Future investigations should be focused on experimental *in vitro* and *in vivo* studies for a better understanding of the antiviral mechanisms of theaflavin-3-gallate metabolite.

Study Highlights

- The best binding affinity was indicated for the interaction of theaflavin-3-gallate ligand towards helicase receptor than to theaflavin-3-gallate and spike protein S1 receptor with the lowest binding affinity.
- Molecular docking studies and the repurposing of approved compounds can cost-effectively accelerate this process.
- Future investigations about antiviral activity of theaflavin-3-gallate should be focused on experimental *in vitro* and *in vivo* studies.

Abbreviations

ACE2: Angiotensin-converting enzyme 2
M^{pro}: Main proteases

PL^{pro}: Papain-like protease
RdRp: RNA-dependent RNA polymerase
SARS-CoV-2: Severe acute respiratory syndrome coronavirus 2

Funding
This work was not supported by any institutes.

Conflict of interest
Not applicable.

Ethical approval
This article does not contain any studies with animals or human participants performed by any of the authors.

Author contributions
Not applicable.

Acknowledgments
Declared none.

References
1. Aljelehawy Q, Mal Allah OR, Sourazur G. Physicochemical properties, medicinal chemistry, toxicity, and absorption of quercetin and its interaction with spike glycoprotein of SARS-CoV-2: Molecular docking. Nano Micro Biosystems. 2022;1(1):32-9. doi:https://doi.org/10.22034/nmbj.2022.163207
2. Aljelehawy Q, Maroufi Y, Javid H, Mohammadi MR, Raji Mal Allah O, Taheri SV, et al. Anticancer, antineurodegenerative, antimicrobial, and antidiabetic activities of carvacrol: recent advances and limitations for effective formulations. Nano Micro Biosystems. 2023;2(1):1-10. doi:https://doi.org/10.22034/nmbj.2023.380207.1009
3. Wong M, Sirisena S, Ng K. Phytochemical profile of differently processed tea: A review. Journal of Food Science. 2022;87(5):1925-42. doi:https://doi.org/10.1111/1750-3841.16137
4. Abudureheman B, Yu X, Fang D, Zhang H. Enzymatic Oxidation of Tea Catechins and Its Mechanism. Molecules. 2022;27(3):942. doi:https://doi.org/10.3390/molecules27030942
5. Shan Z, Nisar MF, Li M, Zhang C, Wan CC. Theaflavin Chemistry and Its Health Benefits. Oxidative Medicine and Cellular Longevity. 2021;2021:6256618. doi:https://doi.org/10.1155/2021/6256618
6. Li Z, Zhu J, Wan Z, Li G, Chen L, Guo Y. Theaflavin ameliorates renal ischemia/reperfusion injury by activating the Nrf2 signalling pathway in vivo and in vitro. Biomedicine and Pharmacotherapy. 2021;134:111097. doi:https://doi.org/10.1016/j.biopha.2020.111097
7. Mostafavi E, Dubey AK, Teodori L, Ramakrishna S, Kaushik A. SARS-CoV-2 Omicron variant: A next phase of the COVID-19 pandemic and a call to arms for system sciences and precision medicine. MedComm (2020). 2022;3(1):e119. doi:https://doi.org/10.1002/mco2.119
8. Nawrot-Hadzik I, Zmudzinski M, Matkowski A, Preissner R, Kęsik-Brodacka M, Hadzik J, et al. Reynoutria Rhizomes as a Natural Source of SARS-CoV-2 Mpro Inhibitors–Molecular Docking and In Vitro Study. Pharmaceuticals. 2021;14(8):742. doi:https://doi.org/10.3390/ph14080742
9. Souza PFN, Lopes FES, Amaral JL, Freitas CDT, Oliveira JTA. A molecular docking study revealed that synthetic peptides induced conformational changes in the structure of SARS-CoV-2 spike glycoprotein, disrupting the interaction with human ACE2 receptor. International Journal of Biological Macromolecules. 2020;164:66-76. doi:https://doi.org/10.1016/j.ijbiomac.2020.07.174
10. Hu Q, Xiong Y, Zhu GH, Zhang YN, Zhang YW, Huang P, et al. The SARS-CoV-2 main protease (M(pro)): Structure, function, and emerging therapies for COVID-19. MedComm (2020). 2022;3(3):e151. doi:https://doi.org/10.1002/mco2.151
11. Jiang Y, Yin W, Xu HE. RNA-dependent RNA polymerase: Structure, mechanism, and drug discovery for COVID-19. Biochemical and Biophysical Research Communications. 2021;538:47-53. doi:https://doi.org/10.1016/j.bbrc.2020.08.116
12. Ran X-H, Zhu J-W, Chen Y-Y, Ni R-Z, Mu D. Papain-like protease of SARS-CoV-2 inhibits RLR signaling in a deubiquitination-dependent and deubiquitination-independent manner. Frontiers in Immunology. 2022;13. doi:https://doi.org/10.3389/fimmu.2022.947272
13. Sommers JA, Loftus LN, Jones MP, 3rd, Lee RA, Haren CE, Dumm AJ, et al. Biochemical analysis of SARS-CoV-2 Nsp13 helicase implicated in COVID-19 and factors that regulate its catalytic functions. Journal of Biological Chemistry. 2023;299(3):102980. doi:https://doi.org/10.1016/j.jbc.2023.102980
14. Cao Y, Li L. Improved protein–ligand binding affinity prediction by using a curvature-dependent surface-area model. Bioinformatics. 2014;30(12):1674-80. doi:https://doi.org/10.1093/bioinformatics/btu104
15. Liu Y, Grimm M, Dai W-t, Hou M-c, Xiao Z-X, Cao Y. CB-Dock: a web server for cavity detection-guided protein–ligand blind docking. Acta Pharmacologica Sinica. 2020;41(1):138-44. doi:https://doi.org/10.1038/s41401-019-0228-6
16. Chauhan M, Bhardwaj VK, Kumar A, Kumar V, Kumar P, Enayathullah MG, et al. Theaflavin 3-gallate

inhibits the main protease (Mpro) of SARS-CoV-2 and reduces its count in vitro. Scientific Reports. 2022;12(1):13146. doi:https://doi.org/10.1038/s41598-022-17558-5
17. Peele KA, Potla Durthi C, Srihansa T, Krupanidhi S, Ayyagari VS, Babu DJ, et al. Molecular docking and dynamic simulations for antiviral compounds against SARS-CoV-2: A computational study. Informatics in Medicine Unlocked. 2020;19:100345. doi:https://doi.org/10.1016/j.imu.2020.100345
18. Giofrè SV, Napoli E, Iraci N, Speciale A, Cimino F, Muscarà C, et al. Interaction of selected terpenoids with two SARS-CoV-2 key therapeutic targets: An in silico study through molecular docking and dynamics simulations. Computers in Biology and Medicine. 2021;134:104538. doi:https://doi.org/10.1016/j.compbiomed.2021.104538
19. Deshpande RR, Tiwari AP, Nyayanit N, Modak M. In silico molecular docking analysis for repurposing therapeutics against multiple proteins from SARS-CoV-2. European Journal of Pharmacology. 2020;886:173430. doi:https://doi.org/10.1016/j.ejphar.2020.173430
20. Khater I, Nassar A. In silico molecular docking analysis for repurposing approved antiviral drugs against SARS-CoV-2 main protease. Biochemistry and Biophysics Reports. 2021;27:101032. doi:https://doi.org/10.1016/j.bbrep.2021.101032
21. Lokhande KB, Apte GR, Shrivastava A, Singh A, Pal JK, Swamy KV, et al. Sensing the interactions between carbohydrate-binding agents and N-linked glycans of SARS-CoV-2 spike glycoprotein using molecular docking and simulation studies. Journal of Biomolecular Structure and Dynamics. 2022;40(9):3880-98. doi:https://doi.org/10.1080/07391102.2020.1851303
22. Patel CN, Jani SP, Jaiswal DG, Kumar SP, Mangukia N, Parmar RM, et al. Identification of antiviral phytochemicals as a potential SARS-CoV-2 main protease (Mpro) inhibitor using docking and molecular dynamics simulations. Scientific Reports. 2021;11(1):20295. doi:https://doi.org/10.1038/s41598-021-99165-4

HOW TO CITE THIS ARTICLE:
Aljelehawy QHA. Docking of helicase, main protease, papain-like protease, and RNA-dependent RNA polymerase of SARS-CoV-2 by theaflavin-3-gallate. Micro Nano Bio Aspects. 2023; 2(3): 38-44.
doi: https://doi.org/10.22034/mnba.2023.410567.1042